# FLAT-PLATE HIGH-FREQUENCY SMALL THRUSTER ON FREE SURFACE

Yutaka Terao
Tokai University, Shizuoka, Japan

The experiments using small propulsion system that uses surface tension rather than gravitational waves to generate thrust is discussed. It consists of a flat-plate fin thruster that rests on a free surface and is driven at over 110 Hz by a small vibration motor and 8-cm-long model achieved speeds is of up to $F_n$ = 0.212 based on the model length Froude number.

**Keywords**: High-frequency propulsion, Surface tension wave, Wave momentum flux

## 1. INTRODUCTION

Waves are not commonly used to create thrust. However, wave-making[1] and wave-devouring[2] propulsion systems generate thrust by employing the radiation force of waves and the relative wave orbital velocity acting on the hydrofoil. Both systems use gravitational waves and it's theories. If the floating body size decreases by less than 10 cm, gravitational waves are no longer dominant, and the waves generated by the small model become surface tension waves. Fig.1 shows the phase velocity of the waves and indicates that if the wavelength is less than 1.7 cm, the surface tension wave phase velocity exceeds the gravitational waves. In ocean engineering or naval structures, this higher-frequency wave zone is not commonly employed in practical applications. This paper discusses experiments on a small propulsion system model ($L_{oa}$ = 80 mm, $B$ = 40 mm, 20 mm slit in the bottom centerline) equipped with a 7000 rpm vibration motor on the deck to know the surface wave making propulsion is possible or not.

In these experiments, as in the gravitational wave-making propulsion system, a high propulsion speed was achieved in the high-frequency tension wave zone. To achieve a much higher speed, an elastic horizontal fin was installed on the aft of the model. A strong flow was observed behind the fin, and the model achieved a high speed. These results indicate the usefulness of the proposed propulsion system.

## 2. MODEL TEST
## 2.1 MODEL

A simple model configuration was adopted because it's easy construction. The hull was constructed from styrene foam with a density $\rho$ of 0.02, and cut using a heat wire in a shape similar to a soap box with a trench under the bottom plane. The cut-out surfaces were waterproofed with paint. Because the model material is styrene, the cutting was easy, but ensuring the precision of the finished dimensions of the model was difficult, necessitating careful cutting. A trench was cut square in the bottom of the model, and the hull was shaped like a catamaran to ensure course stability during the self-propulsion test.
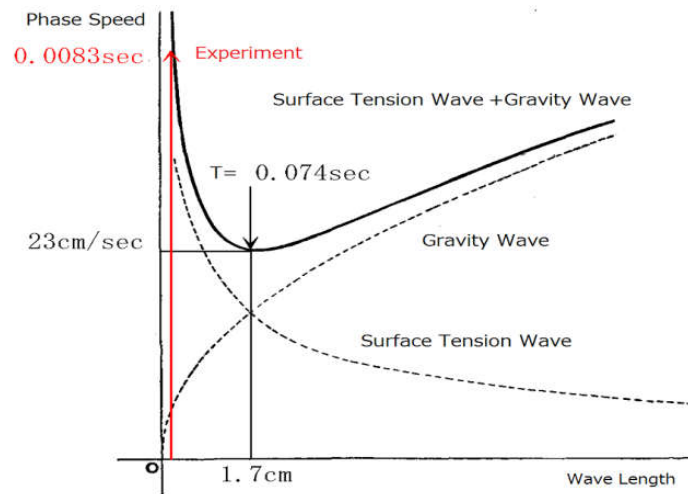
Figure 1. Phase speed as a function of wavelength.

## 2.2 SMALL VIBRATOR

The small vibrator shown in Photo.1 was used in this study. It is a light-weight direct current (DC) vibrator motor that is commonly used in cellular phones. The vibrator has one unbalanced weight installed along the rotating axis, and the high-frequency revolution of the motor produces a centrifugal force that causes vibration. A photo-interrupter type rotation meter was built and used to determine the motor voltage to rotating characteristics rpm/V. In this measurement, a newly developed system based on the PIC16F873A microcontroller was used, and the measurement results are shown in Fig.2. This figure shows that a 1.5 V battery drives the motor at 110 rps and produces a 110 Hz vibration.

Photo.2 shows the micro vibration motor integrated into a circuit consisting of a micro-switch and 1.5 V button-type cell battery to drive the vibrator assembled on a universal base measuring 10 mm × 40 mm. The gross weight of the model is 12 grf (1.22 dyne). Photo.3 shows how the micro forced oscillator was attached to the model during testing.



Photograph 1. Micro vibration motor.



Photograph 2. Circuit of micro forced oscillator, including micro vibration motor, battery, and switch.
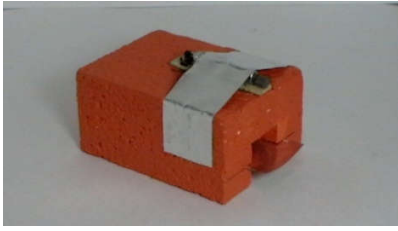
Photograph 3. Model setup during testing.
A flexible horizontal fin was attached to the aft of the model, and the micro forced oscillator was mounted on the model deck.
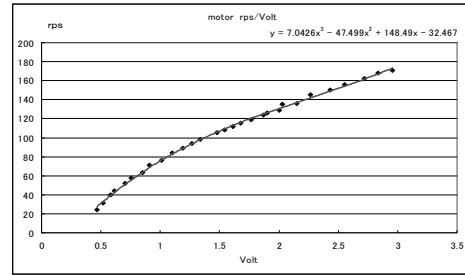


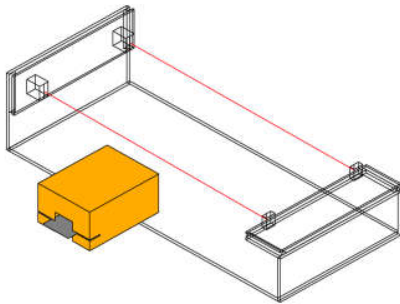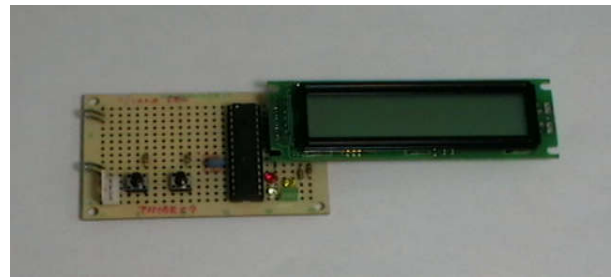Figure 2. Rotational speed of micro motor vs. input voltage.



Figure 3. Schematic of test setup. Infrared (IR) photogates were constructed to measure the model speed.



Photograph 4. Newly designed 1/000 s precision count up stopwatch based on PIC16F873A microcontroller.



Photograph 5. Model measurement setup. The shallow water tank was constructed from acrylic plates. Paper was attached to the tank side plates to intercept extra light. The water depth was 27 mm, and the length and breadth of the tank were 1770 and 540 mm, respectively.

## 2.3 MEASUREMENT SYSTEM

Fig.3 shows the noncontact photogate that was built to measure the forward speed of the model. The measurement system was constructed using two infrared (IR) light-emitting diodes (LEDs) with 40 kHz pulse emissions to set the start and end signals. Two sets of photogates were used to receive the start and end signals and count up the elapsed time between them, representing the time required for the model to pass between the two photogates. To eliminate the effects of wind, a shallow water tank made of acrylic fiber was used, as shown in Photo.5. The depth of the water in the tank was set to 27 mm. To measure the time required for the model to pass between the photogates, a 1/1000 s precision stop watch system was developed using a PIC16F873A controller and a 20 MHz clock, and the forward speed of the model was recorded.

## 2.4 EXPERIMENTAL RESULTS

At a battery voltage of 1.5 V, the model vibration is 110 Hz, as shown in Fig.2, and the forward speed depends on the fin width. A fin made of steel use stainless (SUS) with a thickness of 0.02 mm was installed on the stern of the model at the same height as the surface elevation. A parallel cut was made 10 mm from the bottom surface. The fin was inserted in and glued to the hull. Fig.4 shows the model forward speed plotted against the fin width; the optimal conditions occur when the forward speed reaches a maximum. The maximum forward speed of 0.18 m/s obtained in this test was relatively high in comparison with the model length (0.08 m).

To observe the flow field behind the fin, a bollard pull test was conducted. A video of this test was recorded, and a still from this video is shown in Photo.6. In this case, the vibration motor was installed on the upper part of the fin. A strong flow formed from the trailing edge of the fin, and a big wave front formed behind the fin. Photo.7, which was taken using a strobe light, shows the wave pattern around the square hull. When this photograph was taken, a surface tension wave had also formed around the hull, but at the aft of the hull and behind the fin, more complex and higher waves were observed.

The jet flow caused by the beating motion of the fin near the free surface significantly contributed to the thrust force generated on the high-frequency vibration fin. As shown in the appendix, the surface tension wave propulsion effect was rather low. In the many experiments conducted on the same small vibrator without a fin, the forward speed is very slow and did not match that achieved with the fin. Moreover, observations revealed that a strong jet flow formed when the high-frequency vibration fin was switched on, even if the vibration frequency was changed. To investigate the frequency dependence of the jet flow formation, power was supplied from outside of the model with an umbilical cable. The voltage was varied from 1 to 3 V, corresponding to a forced frequency of 90–190 Hz, and a strong jet flow was observed at each voltage.
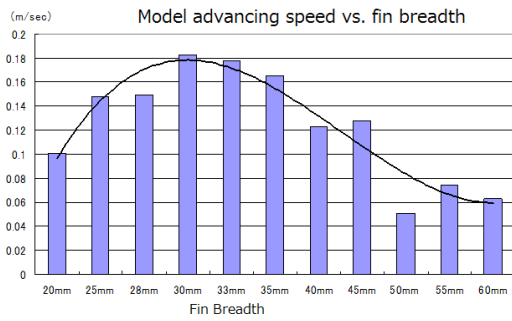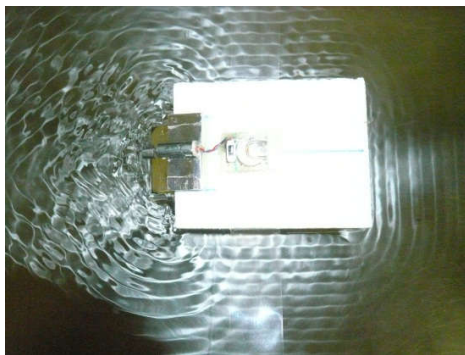
Figure 4. Model forward speed plotted against fin width with fin length of 20 mm.



Photograph 6. Flow field during bollard pull test. Steady surface elevation and strong jet flow were observed at the aft of the fin. Large air bubbles were thrown with strong flow.



Photograph 7. Surface tension wave pattern generated by high-frequency vibration system. Model was moored by transparent tape.
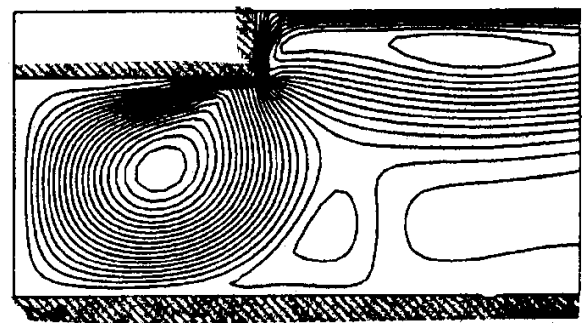


Figure 5. Calculated sample of acoustic streaming[3].

# 3. CONCLUSION

In naval architecture, gravitational waves are very common, and their high-frequency surface tension wave region is not currently an area of interest. Therefore, when we began this study, we found no reports or investigations concerning such phenomenon. However, after the experiments in this study were conducted, we discovered that similar phenomena have been reported in studies on acoustic flow[3].

Acoustic flow is flow caused by the acoustic pressure that occurs on a vertical vibrating surface when an ultrasonic device is submerged in a fluid. Additionally, a strong flow is generated in the direction tangential to the acting face. The ultrasonic frequency is near 40 kHz, but the frequency of the vibration of the fin in this case is less than 0.1 kHz. Furthermore, the direction of the fin vibration is the same as that in the ultrasonic vibration device discussed in this paper.

The figure is the numerical analysis of this acoustic problem and discusses a phenomenon that accompanies ultrasonic vibration. An example of a calculated acoustic flow field is shown in Fig.5. This figure shows that the flow caused by the ultrasonic vibration includes a strong circular flow started from the rear edge part. This phenomenon is regarded to be the same as that investigated in the present study, but it must be considered in more detail in future works.

## REFERENCES

1) Longuet-Higgins, M. S. :   The mean force extracted by waves on floating or submerged bodies with application to sand bars and wave power machines,  Proc.  R.  Soc.  London.  A.  352,  1977,p463

2) Yutaka Terao; The floating object which drift against the wave- Possibility of the   wave propulsion system-,1982,KSNAJ No.184, pp51-54

3) Charles Thompson, et.al: Acoustic streaming generated by an oscillating surface, Frontiers of nonlinear Acoustics; Proc. 12th ISNA,1990, pp365-370

# APPENDIX

## A1. THRUST GENARATION BY RADIATING SURFACE WAVE

Surface tension waves can be described by the equation

$$p_{z=\eta} - p_0 = -\frac{\alpha \partial^2 \eta}{\partial x^2} , \tag{1}$$

where $\alpha$ is the surface tension and $\eta$ is the wave height. The kinematic equation is then

$$\varphi_t + \frac{1}{2}u^2 + \frac{p}{\rho} + g\eta = \frac{\alpha}{p_0}\frac{\partial^2 \eta}{\partial x^2} . \tag{2}$$

Equations (1) and (2) can be linearized as

$$\eta_t = \varphi_z \tag{3}$$

$$\varphi_t = -g\eta + \frac{\alpha}{p_0}\frac{\partial^2 \eta}{\partial x^2} . \tag{4}$$

The following solutions satisfy equations (3) and (4):

$$\eta = \sum_k A_k e^{i\omega t} \sinh k(h+z) \tag{5}$$

$$\varphi = \sum_k B_k e^{i\omega t} \sinh k(h+z) . \tag{6}$$

Then

$$\frac{\partial^2 A_k}{\partial t^2} = -(gk + \frac{\alpha}{\rho}k^3)\tanh kh A_k \tag{7}$$

$$\omega = \sqrt{(gk + \frac{\alpha}{\rho}k^3)\tanh kh} . \tag{8}$$

In this case, $h >> 0$, and

$$\omega = \sqrt{gk + \frac{\alpha}{\rho}k^3} . \tag{9}$$

The region in which surface waves are dominant is given by

$$k_m = \sqrt{\frac{g\rho}{\alpha}} \tag{10}$$

$$\lambda_m = 1.7(cm) . \tag{11}$$

The phase speed $C$ is defined as

$$C = \sqrt{\frac{\omega}{k}} = \sqrt{\frac{g}{k}}\sqrt{1 + \frac{k^2}{k^2_m}} \tag{12}$$

$$c_m = \sqrt{\frac{2g}{k_m}} = 23(cm/\sec) \qquad at \quad k = k_m . \tag{13}$$

Following the momentum theory by Longuet-Higgins[1], the thrust force can be derived from the radiating surface tension wave. The energy $E_s$ of the surface tension wave is

$$E_S = \frac{A}{2}\frac{\alpha}{2}k^2\eta^2 , \tag{14}$$

and the surface tension wave group velocity $C_g$ is

$$kh >> 1 , \text{ and } \tanh kh = 1 \tag{15}$$

$$C_g = \frac{3}{2}C . \tag{16}$$

Therefore, the phase speed $C$ is

$$C = (\frac{2\pi\alpha}{\rho\lambda})^{1/2} = \left(\frac{\alpha k}{\rho}\right)^{1/2} . \tag{17}$$

The thrust produced by the radiating surface tension wave   of the height   A   is then given as

$$F = E_s / C_g$$

$$= \frac{\frac{1}{2}A\frac{1}{2}\alpha k^2\eta^2}{\frac{3}{2}(\frac{\alpha k}{\rho})^{1/2}} \tag{18}$$

$$= \frac{A}{6}(\alpha k^3\rho)^{1/2}\eta^2$$

## A2. PURE SURFACE TENSION WAVE MAKING PROPULSION SYSTEM

Some experiments were conducted without a fin in the floating body. The bow down trim was 30 mm, as shown in Photo.8. The vibration motor was used as well as in the present study. In this case, a forced vibration made directly the hull vibration and surface tension waves were generated as shown in Photo.9. In this case, the hull moved to the right in Photo.9. The surface tension wave height was a few millimeters, and it was difficult to distinguish whether the bow or the stern wave had a greater height. This small difference of the surface tension wave height, bow and stern wave, caused poor propulsion efficiency and also showed slow advanced speed performance.

If the direction of the diverging surface tension wave and height can be controlled freely, a thrust force

will be larger than that as shown in Photo.9. Our forced oscillator is composed one unbalanced DC motor vibrating system and quite simple but at the same time, vibrate the hull with 6-degree of the hull motion. And undesired hull motion causes plane-diverging waves. This is reason why the low forward speed achieved by the surface tension wave-making propulsion system.

However, with a horizontal fin, the height of the stern surface tension wave may surpass that of the bow surface tension wave, as shown in Photo.7. The combined effect of this and the effect of the fin jet flow allow the high speed performance of the floating body.

For the simple model shown in Photo.8 and Photo.9, the forward speed is only several centimeters per second, and the course stability is quite poor. Therefore, while there is hydrodynamic interest in this model, its application as a small hull thruster would be ineffective.



Photograph 8. Surface tension wave making propulsor. Model advancing direction is right of the photo.
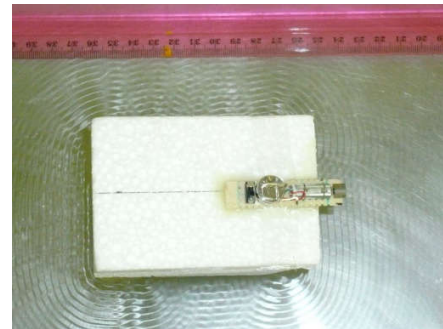


Photograph 9. Generated surface tension waves with model running condition. The model moving direction is right.